Metamaterial Design Strategy for Re-usable, Universal Energy Absorption

Jack E. Pechac[a], Michael J. Frazier[a]

[a]*Department of Mechanical and Aerospace Engineering, University of California, San Diego, California 92093, USA*

ARTICLE INFO

ABSTRACT

This article proposes a design strategy for two-dimensional, multi-stable cellular materials which leverages local rotational degrees of freedom in support of universal energy absorption. The approach aligns the rotation centers of two layers of identical patterning but opposite chirality such that the relative angular displacement accompanying any in-plane deformation facilitates local snap-through events which contribute to the global (hysteretic) energy absorption performance. The rotation symmetry of the underlying (quasi-)crystalline layers governs the directionality of the energy absorption capacity. Moreover, cellular materials emerging from the proposed strategy possess an absorption capability for all loading modes – tension, compression, and shearing. Simulations reveal the energy absorption capacity and the isotopy thereof for several cellular bi-layers as well as the impact of key tuning parameters. The cellular materials constructed following the proposed design strategy fill the need for omni-directional, multi-modal (i.e., universal) energy absorption in a low-density, tunable, and re-usable platform.

1. Introduction

Energy-absorbing materials [1] are ubiquitous in nature [2] and engineering applications demanding, e.g., shock/impact mitigation and stress redistribution/relief. A generic loading-unloading cycle generates a characteristic hysteresis in the load-displacement diagram which, by the enclosed area, quantifies the absorbed energy. While conventional energy-absorbing materials (e.g., polymers, gels, and foams) have their advantages, the material-specific composition/microstucture and absorption mechanism manifest inherent limitations as well. Compared to cellular materials – of which foams are the most widespread – polymers and gels are dense and exhibit a short deformation range for a given peak stress, limiting the energy absorption capacity. However, the pseudo-stochastic nature of the typical foam microstructure hinders predictive modeling and is difficult to control during the manufacturing process, potentially yielding non-uniform properties [3–5]. Moreover, in order to elicit the desired hysteretic behavior, certain cellular materials utilize destructive absorption mechanisms (e.g., plastic deformation [6] and fragmentation [7, 8]) which sacrifices re-usability. Among several desirable characteristics, the ideal energy-absorbing material is low-density, and delivers predictable and repeatable performance under general loading.

Over the past decade, researchers have designed and realized mechanical metamaterials [9–11] whose extreme/unusual mechanics [12–16] emerge from an engineered, highly-tunable microstructure rather than the composition. In the context of energy absorption, cellular metamaterials [17–19] inherit the low density of foams, while enhancing predictabililty and re-usability with ordered microstructures that remain elastic during

*corresponding author: mjfrazier@ucsd.edu
ORCID(s): 0000-0003-3801-2958 (M.J. Frazier)

the loading-unloading process. Although, currently, the energy-absorption capacity is not comparable to conventional materials, cellular metamaterials may serve a complementary role in applications.

A review of the metamaterial literature reveals snap-through, e.g., of buckled/buckling beams [20–32], conical shells [33], or antagonistic arrays of magnets [34, 35], to be a well-utilized mechanism to elicit a hysteretic response. Loading causes snapping elements at the microstructural level to transition from one energetically stable equilibrium configuration to another; thus, snap-through implies multi-stability. Although structurally 1D–3D, most of the above-cited cellular metamaterials are functionally one-dimensional, exhibiting a significant energy absorption capacity for loading along a single axis [20–28, 34], or are subjected to uni-axial loading along equivalent axes of symmetry [29, 30, 33]. Moreover, despite the complex loading of real-world environments, from the native (i.e., ground) configuration, current metamaterial designs accommodate simple load cases, i.e., loading in tension [20], compression [22–26, 29–31, 33], or shear [32, 35], exclusively, and thus limit the energy absorption capability. The constraints on loading direction and variant is a consequence of utilizing snapping elements that are similarly restricted in their activation. While the metamaterial platform has achieved predictable, tunable, and re-usable energy absorption, a pressing challenge lies in devising a strategy for constructing cellular metamaterials with universal energy absorption capability: effective energy absorption from loading (i) along any axis and (ii) of any variant.

Here, we propose an alternative strategy based on snap-through transitions in the rotational degrees of freedom to create cellular metamaterials capable of universal energy absorption. We numerically analyze the absorption capabilities of various 2D (quasi-)crystalline metamaterials,
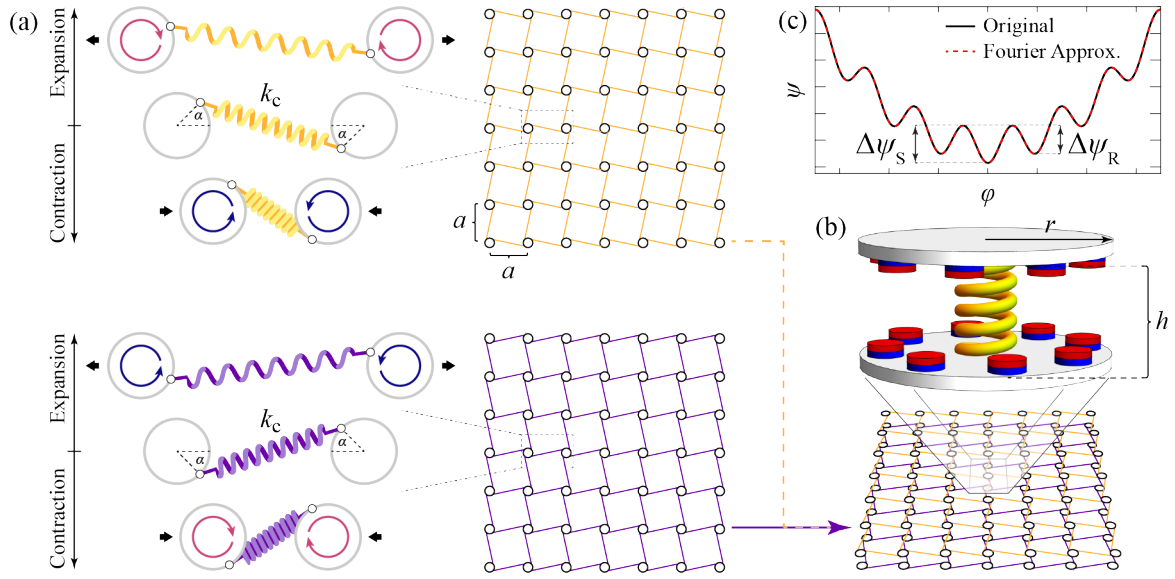
Figure 1: Construction of Multi-stable Cellular Materials. (a) Two lattices of identical arrangement but opposite chirality are aligned and corresponding rotation centers constrained to exhibit a common in-plane translation and permit a relative rotation, φ. Due to the opposing chirality, deforming the cellular bi-layer generates a non-zero φ. (b) Paired rotation centers, represented by discs, interact via magnetic elements along the perimeter and a torsional spring. (c) The corresponding on-site potential function, $\psi(\varphi)$, is symmetric and features multiple minima associated with (meta-)stable configurations. The barrier to transition to the first meta-stable state is labeled $\Delta\psi_S$, while the reversion barrier is $\Delta\psi_R$. Simulations utilize a (relatively) computationally inexpensive 2nd-order Fourier approximation of the magnetic component of the potential, $\psi_m(\varphi)$.

demonstrating a flexibility of construction. We also observe a direction-dependent energy absorption reflecting the rotational symmetry of the arrangement. Such cellular metamaterials expand the capabilities of current design strategies by permitting energy absorption from a broader spectrum of loading conditions and may be a viable alternative/complement to stochastic foams due to enhanced predictability, tunability, and re-usability. While energy absorption is a process encompassing both storage and dissipation, for brevity, we narrow our report to the energy storage component, reserving consideration of the dissipative contribution to a later study.

2. Structure and Methods

2.1. Design Strategy

In general, each cellular material design aligns a pair of two-dimensional lattices of identical (quasi-)periodic arrangement but opposite chirality such that any in-plane deformation of the resulting bi-layer is accommodated by a relative angular displacement, $\varphi = \varphi_t - \varphi_b$, between corresponding rotation centers in each layer (Figs. 1a,b). As the system deforms, a rigid rod through the common axis of rotation maintains the alignment, ensuring that paired centers of rotation undergo identical in-plane displacement, $\mathbf{u} = \{u_x, u_y\}$ while preserving independent rotations. Similar chiral [36, 37] and anti-chiral [38] cellular bi-layers have been theoretically, numerically, and experimentally

investigated in the context of directional auxeticity, but lacked the critical multi-stability for exploration of energy absorption aspects. In the present study, paired rotation centers, represented by two concentric discs of mass, m, radius, r, and separated by an inter-layer spacing, h, facilitate the formation of multi-stable elements when the perimeter of each is decorated with n permanent magnets of opposing polarization (Fig. 1b). Among other parameters, magnetic interactions are affected by the dimensions of each magnet; however, for simplicity and without loss of generality, we idealize each magnet as a point dipole moment $\mathbf{m}_i$. Accordingly, the multi-stable potential function of the magnetically-coupled discs is given by $\psi_m(\varphi) = -\sum_{i=1}^{n}\sum_{j\neq i}^{n} \mathbf{m}_i \cdot \mathbf{B}_{ij}(\varphi)$, where $\mathbf{B}_{ij}(\varphi)$ is the magnetic field produced by $\mathbf{m}_j$ at the location of $\mathbf{m}_i$. The resulting potential landscape is symmetric about $\varphi = 0$ with infinite ground state configurations, $\varphi = p\varphi_0$, $p \in \mathbb{Z}$, appearing at regular intervals. If practical considerations preclude the use of magnets, then a similar multi-stability may be achieved mechanically by substituting the magnets for sinusoidal elastic embossments along the perimeter of each disc, i.e., the angular equivalent of the translation-based multi-stable units described in Ref. [27] [Fig. S1 of Supporting Information (SI)]. To promote recoverability, we introduce a torsional spring of stiffness, k_t, which penalizes φ according to $\psi_t(\varphi) = k_t\varphi^2/2$ such that the total on-site potential, $\psi = \psi_m + \psi_t$, possesses a single ground state, $\varphi = 0$, and a finite number of meta-stable states of increasing energy for

increasing $|\varphi|$ (Fig. 1c).

The multi-stable elements, arranged in a (quasi-)crystalline pattern and elastically connected, form a cellular bi-layer. In particular, linear springs of stiffness, k_c, couple co-planar discs in neighboring elements by attaching to their perimeter via pin joints (Fig. 1a). For the top (bottom) discs of coupled elements, the joints are situated at an angle α ($-\alpha$) from the line through the center of each disc forming a chiral lattice. Apparently, any loading-induced deformation of the cellular material which changes the center-to-center distance, a, between elements involves a change in length in the interaction springs and a relative rotation between the discs comprising the multi-stable elements. Thus, we expect φ and snap-through events to increase where the magnitude of the effective dilation is greatest. Following snap-through, upon settling into a meta-stable state, energy is stored in the local and non-local elastic/magnetic components of the bi-layer. Since, as demonstrated in the following, the deformation may stem from in-plane tensile and compressive loading along any axis as well as in-plane shear loading, the (quasi-)crystalline cellular metamaterial emerging from the proposed design strategy possesses an universal energy-trapping capability.

The mass-spring lattices discussed in this article are a computationally efficient simplification of more practical chiral beam structures (Fig. S1 of SI). However, the lack of a bending rigidity in the simplified construction causes lattices to be susceptible to collapse, especially when loaded in compression or shear. Consequently, for stability, a bending rigidity is re-introduced by mounting bi-layers upon non-chiral, straight-beam lattices of identical arrangement.

2.2. Simulation

In order to demonstrate the proposed strategy for universal energy absorption, we analyze *in silico* the energy absorption performance of various (quasi-)crystalline cellular bi-layers subject to quasi-static, in-plane loading. The material response to dynamic loading will be explored in a separate article. To that end, regardless of lattice arrangement, we consider bi-layer samples approximately $20a \times 20a$ in dimension and loaded at various orientations, θ. Specifically, as illustrated in Fig. 3a for a square sample, the multi-stable elements are placed at the lattice points but only those within the $20a \times 20a$ region are elastically connected to form the sample; the remainder are discarded from the model. Regarding the impact of the sample dimensions on the material performance, preliminary studies showed the results from $20a \times 20a$ samples to be qualitatively similar to those obtained at greater computational cost from $60a \times 60a$ samples. The load, applied to the top boundary of the rectangular sample while the bottom remains fixed, is based on a symmetric triangle wave (see SI). While bi-axial, twisting, and concentrated loads – whether quasi-static or dynamic – are of practical relevance, for brevity, simulations concern only uni-axial tension and compression, and shear, under quasi-static conditions at various orientations. In general, the (quasi-)crystalline

samples do not possess smooth boundaries; therefore, for loading purposes, elements within $0.9a$ of the rectangular boundary are treated as the boundary elements. For computational economy, we approximate $\psi_m(\varphi)$ by a 2nd-order Fourier expansion. All dimensionless material and geometric parameters are listed in the SI.

3. Results and Discussion

3.1. Energy-trapping Mechanism

Figure 2 depicts the response of an initially undeformed cellular bi-layer with square arrangement to separate loading-unloading cycles in tension, compression, and shear, respectively (Movie S1 of SI). In particular, through snapshots, Fig. 2 shows the lattice deformation and phase (i.e., relative rotation) distribution at different instances within a cycle. Auxetic effects due to chiral interactions between multi-stable elements are apparent in the deformation. In addition, snap-through phase transitions indicative of energy absorption occur irrespective of loading mode. The sign of the phase is opposite that of the local effective dilation. As $|\varphi|$, generally, increases with the magnitude of the effective dilation, snap-through initiates along the unconstrained boundaries of the structure and propagates toward the interior. Upon removal of the load, the bi-layer maintains a residual deformation as well as a smooth phase gradient as a consequence of the multiple possible states into which snapped elements may settle. Upon unloading, we find that bi-layers whose snapping elements possess an optimum number of magnets are less likely to have those elements return to the zero-energy ground configuration (see Sec. 3.3), an effect which increases the overall energy absorption.

Figure 2 also plots the force-displacement response for each loading case with labels for the corresponding configurations depicted in the snapshots. The curves illustrate the familiar hysteretic behavior associated with energy absorption as measured by the area of the enclosed region, $E = \int f \, du$. In particular, during the loading phase, the tension and compression cases show a well-defined plateau region – which is tunable in the metamaterial platform – over which most of the energy-absorbing snapping events occur. Continued loading stimulates further, intermittent snapping among progressively smaller sets of elements as the system saturates. In the shear case, snapping begins early in the loading phase and proceeds at a relatively constant rate, preventing definite plateau force. Although simulated samples include a viscous damping force in order to attenuate small-amplitude oscillations (assisting the quasi-static analysis), its influence is sufficiently small that the hysteresis energy closely approximates the total energy stored in the sample's magnetic/elastic constituents. The proposed design strategy does not exploit destructive mechanisms that hinder the re-usability of the cellular material (e.g., plastic deformation, fracture), therefore the stored energy is recoverable.
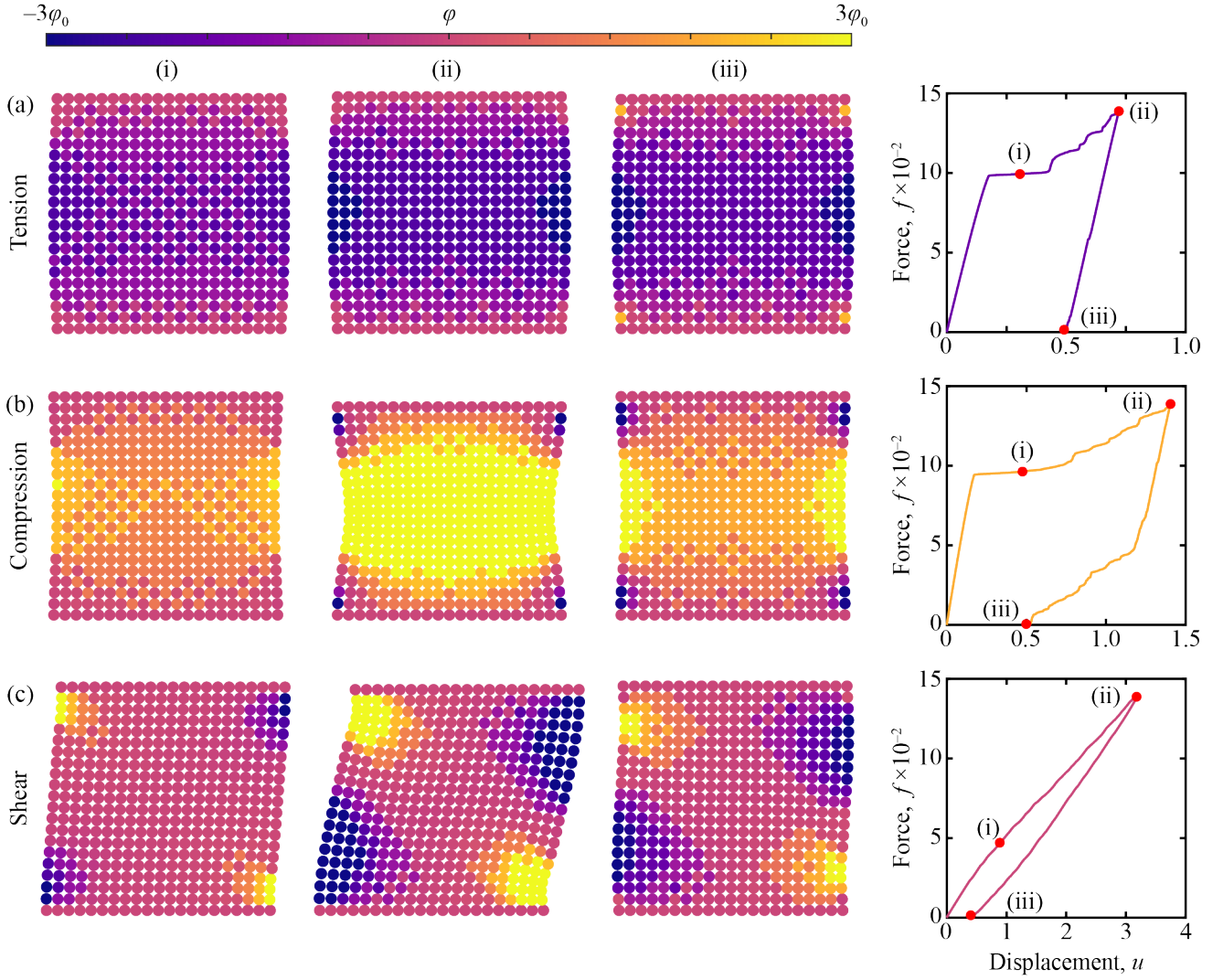
Figure 2: Loading the Cellular Material. (a) The evolution of in-plane displacement and phase distribution in a square cellular bi-layer subject to quasi-static loading in (a) tension, (b) compression, and (b) shear. The phase distribution shows the transition to progressively higher meta-stable states (i) during loading, (ii) at peak loading, and (iii) following unloading. The corresponding hysteresis of the force-displacement diagram is a testament to the energy absorption capability of the bi-layer under each loading condition.

3.2. Symmetry and Isotropy

The hysteretic response exhibited by the square lattice in Fig. 2 is not limited to a single loading direction; regarding tension/compression, the energy-trapping capability persists for loading along axes of arbitrary orientation, θ. Similarly, loading any two parallel planes in shear will generate a hysteresis. These results stem from the internal chiral architecture of the cellular material which guarantees that any deformation of the bi-layer is accommodated by a non-zero φ, promoting snap-through. Moreover, the chiral feature permits energy absorption irrespective of the underlying lattice arrangement: crystalline *or* quasi-crystalline. Here we examine crystalline square and triangular lattices, as well as quasi-crystalline P3 Penrose [39] and Ammann-Beenker (AB) tilings (Fig. S of SI).

Figure 3b plots the direction-dependent energy absorption, $E(\theta)$, for various (quasi-)crystalline cellular materials loaded in tension, compression, and shear. Apparently, loading bi-layers at particular orientations elicits a more efficient absorption response. These arrangement- and loading-specific orientations correspond to a lower effective stiffness, leading to larger displacements which promote absorption. Naturally, the directional response of each bi-layer is directly related to the rotational symmetry of the component lattices. While quasi-crystals lack translational symmetry, they possess a local rotational symmetry which may exceed those of traditional crystals – a feature which may elicit a more isotropic response. The square, triangular, and AB samples exhibit a directional energy absorption with four-, six-, and eight-fold rotational symmetry, respectively, which is consistent with that of the direct lattice of the internal architecture. Seemingly to the
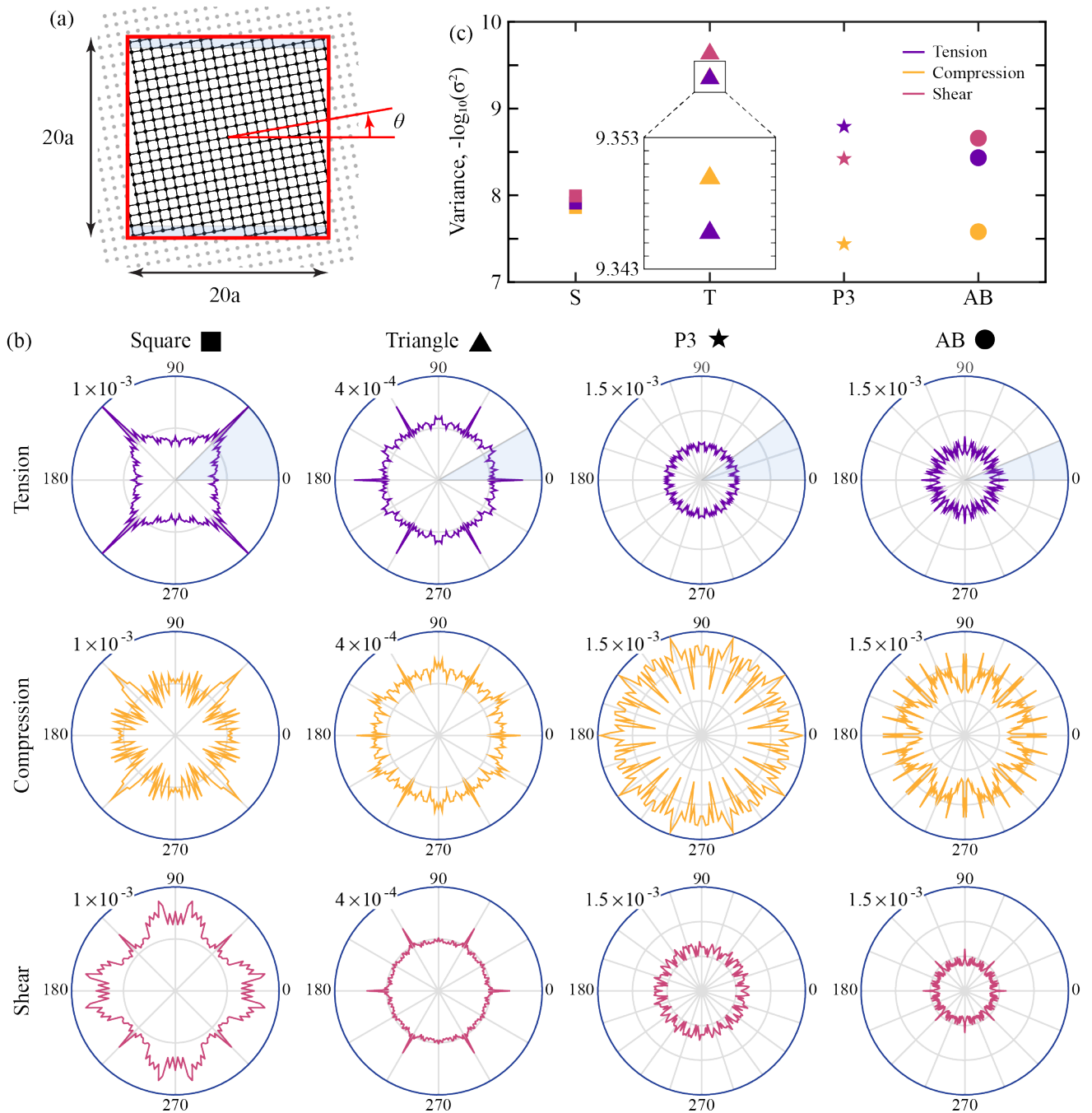
Figure 3: Rotational Symmetry of Cellular Bi-layers. (a) Sample of a cellular bi-layer with underlying square lattice at orientation, θ, loaded along opposing boundaries (blue). (b) The direction-dependent energy absorption of various (quasi-)crystalline lattices. (c) A comparison of the variance amongst the different lattice arrangements, a measure for effective isotropy.

contrary, the Penrose bi-layer, characterized by an internal architecture with fifth-order rotational symmetry, produces an energy diagram with ten-fold rotational symmetry. This is due to an additional five axes of mirror symmetry that complete the D_5 dihedral group of the lattice. As an odd dihedral group, each of the ten symmetries in the group gives an inner automorphism which results in the same energy absorption. [40].

In practical settings where the loading direction is unpredictable or changing, it may be beneficial for materials to exhibit an energy absorption capacity that is isotropic. Nevertheless, energy diagrams with higher order rotational symmetry – indicating identical energy trapping for a greater number of loading directions – do not imply isotropic energy absorption for identical loading as effectiveness varies with θ. A truly isotropic material would have no variation in
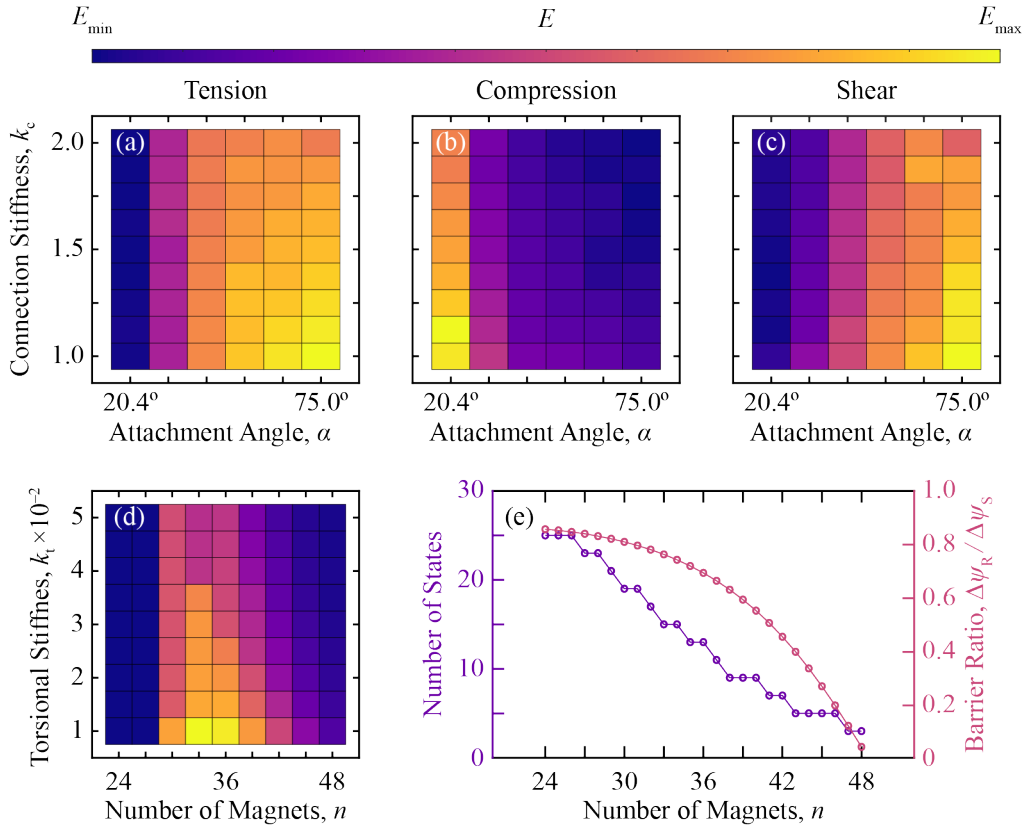
Figure 4: Dependence of energy absorption on local and non-local parameters. Energy absorption, E, varies with the attachment angle α and the non-local connection stiffness k_c in (a) tension, (b) compression, and (c) shear. (d) Locally, the torsional stiffness k_t and the number of magnets on a disc n alter the local potential which affects absorption. (e) The number of stable states and the ratio of the energy barriers for reversion and transition vary with the number of magnets, characterizing the local potential landscape.

its energy absorption capacity with respect to orientation and, hence, produce a circle in a polar plot. Here, in order to quantify the directionality of energy absorption of various (quasi-)crystalline cellular bi-layers, we measure the variance, $\sigma^2 = \sum^N [E(\theta_i) - E_{avg}]^2/(N-1)$, of the energy plots in Fig. 3b, which approaches zero as the response becomes isotropic. Figure 3c summarizes the results, displaying relatively tight clusters for crystalline arrangements as σ^2 is nearly independent of loading mode. On the other hand, for quasi-crystalline arrangements, greater disparities in variance are observed, especially in compression.

3.3. Exploring the Design Parameter Space

The metamaterial platform facilitates the customization of the load-displacement curve and, thus, the energy absorption through adjustments to the material and geometric parameters defining the internal architecture, representing, potentially, a vast design space. In order to demonstrate the impact of certain design choices on the bi-layer absorption performance, we explore the parameter space of a bi-layer with square arrangement at orientation, $\theta = 0°$. Simulations apply an identical, quasi-static

loading-unloading schedule to bi-layers characterized by unique architectures and measure the corresponding absorption. Figures 4a–d plot the simulation results, revealing the combination of design parameters – classified as local (e.g., k_t and n) or non-local (e.g., k_c and α) type – which maximize/minimize the absorption for a particular mode of loading.

In addition to lattice arrangement, the non-local design parameters control the receptibility of the bi-layer to energy absorption by specific modes of loading. Figures 4a–c, respectively, plot the absorption for bi-layers under tension, compression, and shear as a function of α and k_c. Naturally, $\alpha = \{0°, 180°\}$ (not shown) destroys the lattice chirality and, consequently, the ability to stimulate snap-through. As illustrated in Figs. 4a,b, for increasing α, the energy absorption capability of the bi-layer improves (declines) when loading in tension (compression). This can be understood by observing that, for loading in tension (compression), the maximum possible relative rotation – considering only the alignment of interaction springs – follows $|\varphi_{max}| = 2\alpha$ $(|\varphi_{max}| = 360° - 2\alpha)$; thus, increasing α presents more (fewer) opportunities for snap-through. In shear (Fig. 4c), the trend is similar to

that of the tensile loading condition. This is because the local compaction produced by shear loads (Fig. 2c) is restricted by contact between neighboring discs while the local expansion is unincumbered; therefore, design choices that encourage absorption in tension have a similar effect in shear. In general, as k_c increases, less energy is absorbed as the bi-layer deformation and, consequently, snap-through events are diminished.

The local design parameters shape the on-site energy landscape responsible for snap-through, a critical effect for establishing a hysteresis in the load-displacement curve. Figure 4d plots the energy absorption of the cellular bi-layer (in tension) as a function of the number of magnets, n, and the torsional stiffness, k_t, where an extremum at ($n = n_c, k_t$) = $(33, 10^{-2})$ suggests an optimum combination of these parameters which maximizes the absorption. This can be understood by observing that as n moves away from the critical value, n_c, the absorption tends toward zero since either the barrier, $\Delta\psi_S$, becomes prohibitively high for the loading to stimulate snap-through ($n < n_c$) or the barrier, $\Delta\psi_R$, becomes vanishingly small such that (non-)local affects more effectively restore transitioned elements to low-energy configurations ($n > n_c$). Naturally, as the torsion spring resists the relative rotation of paired discs, increasing k_t inhibits snap-through which, in turn, diminishes the absorbed energy. Figure 4e summarizes for a given k_t, showing that as n increases, the number of meta-stable states (i.e., the opportunity for snap-through) and the depth of corresponding on-site energy wells (i.e., the resistance to return snap-through) simultaneously decrease.

4. Conclusion

In summary, this article proposes a strategy to construct two-dimensional, cellular metamaterials for re-usable, universal energy absorption. The strategy assembles a cellular bi-layer from two lattices of identical arrangement but opposite chirality and coupled elasto-magnetically through the aligned rotation centers to form multi-stable elements. Subsequently, any deformation of the bi-layer in response to general mechanical loading – tension/compression along any axes and shearing of any pair of parallel planes – stimulates snap-through, leading to hysteresis in the load-displacement curve indicative of energy absorption. The strategy is amenable to a number of (quasi-)periodic arrangements, demonstrating its flexibility. Here, example bi-layers composed of square, triangular honeycomb, P3 Penrose, and Ammann-Beenker chiral lattices are loaded quasi-statically, revealing a direction-dependent energy absorption reflecting the rotational symmetry of the lattice arrangement. We expect anti-chiral architectures to yield similar results.

A number of parameter studies illuminated the impact of material and geometric design choices on the absorption. In particular, for a given loading-unloading schedule, the relationship between absorption and the number of magnets is complex: too few magnets manifest large energy barriers, hindering snap-through while too many magnets risks eliminating meta-stable states altogether. Nevertheless, replacing the magnets with elastic embossments (Fig. S1 of SI) voids this trade-off.

The metamaterial platform provides improved predictability and tunability in the performance over stochastic foams and realizes an energy absorption capability without relying on destructive mechanisms, promoting re-usability. Here, we present the metamaterial response to quasi-static loading such that the absorption is chiefly the energy stored in the bi-layer elasto-magnetic potentials; the additional energy dissipated by, e.g., harmonic loading will be considered elsewhere. In addition, while we apply the proposed strategy toward the construction of planar metamaterials, the construction and characterization of curved surfaces – a logical extension into the third dimension – represents a potential research direction.

Acknowledgments

Conflict of Interest

The authors declare that they have no conflict of interest.

References

[1] G. Lu, T. Yu, Energy Absorption of Structures and Materials, Woodhead Publishing, Cambridge, England, 2003.

[2] Y. Zhang, O. Paris, N. J. Terrill, H. S. Gupta, Uncovering three-dimensional gradients in fibrillar orientation in an impact-resistant biological armour, Sci. Rep. 6 (2016) 26249.

[3] M. Avalle, G. Belingardi, A. Ibba, Mechanical models of cellular solids: Parameters identification from experimental tests, Int. J. Impact Eng. 34 (2007) 3–27.

[4] L. J. Gibson, M. F. Ashby, Cellular Solids: Structure and Properties, 2nd ed., Cambridge University Press, New York, New York, 1999.

[5] M. F. Ashby, A. Evans, N. A. Fleck, L. J. Gibson, J. W. Hutchinson, H. N. G. Wadley, Metal Foams: A Design Guide, Elsevier Science, Burlington, Massachusetts, 2000.

[6] A. G. Evans, M. Y. He, V. S. Deshpande, J. W. Hutchinson, A. J. Jacobsen, W. B. Carter, Concepts for enhanced energy absorption using hollow micro-lattices, Int. J. Impact Eng. 37 (2010) 947–959.

[7] L. R. Meza, S. Das, J. R. Greer, Strong, lightweight and recoverable three-dimensional ceramic nanolattices, Science 345 (2014) 1322–1326.

[8] A. G. Izard, J. Bauer, C. Crook, V. Turlo, L. Valdevit, Ultrahigh energy absorption multifunctional spinodal nanoarchitectures, Small 15 (2019) 1903834.

[9] J.-H. Lee, J. P. Singer, E. L. Thomas, Micro-/Nanostructured mechanical metamaterials, Adv. Mat. 24 (2012) 4782–4810.

[10] K. Bertoldi, V. Vitelli, J. Christensen, M. van Hecke, Flexible mechanical metamaterials, Nat. Rev. Mater. 2 (2017) 17066.

[11] D. M. Kochmann, K. Bertoldi, Exploiting microstructural instabilities in solids and structures: from metamaterials to structural transitions, Appl. Mech. Rev. 69 (2017) 050801.

[12] R. S. Lakes, Foam structures with a negative Poisson's ratio, Science 235 (1987) 1038–1040.

[13] L. Cabras, M. Brun, Auxetic two-dimensional lattices with Poisson's ratio arbitrarily close to -1, Proc. R. Soc. A. 470 (2014) 20140538.

[14] T. A. M. Hewage, K. L. Alderson, A. Alderson, F. Scarpa, Double-negative mechanical metamaterials displaying simultaneous negative stiffness and negative Poisson's Ratio Properties, Adv. Mat. 28 (2016) 10323–10332.

[15] R. Hedayati, A. M. Leeflang, A. A. Zadpoor, Additively manufactured metallic pentamode meta-materials, Appl. Phys. Lett. 110 (2017) 091905.

[16] L. Cabras, M. Brun, D. Misseroni, Micro-structured medium with large isotropic negative thermal expansion, Proc. R. Soc. A. 475 (2019) 20190468.

[17] E. B. Duoss, T. H. Weisgraber, K. Hearon, C. Zhu, W. Small, T. R. Metz, J. J. Vericella, H. D. Barth, J. D. Kuntz, R. S. Maxwell, C. M. Spadaccini, T. S. Wilson, Three-dimensional printing of elastomeric, cellular architectures with negative stiffness, Adv. Funct. Mater. 24 (2014) 4905–4913.

[18] K. Fu, Z. Zhao, L. Jin, Programmable granular metamaterials for reusable energy absorption, Adv. Funct. Mater. 29 (2019) 1901258.

[19] J. Mueller, K. H. Matlack, K. Shea, C. Daraio, Energy absorption properties of periodic and stochastic 3D lattice materials, Adv. Theory Simul. 2 (2019) 1900081.

[20] A. Rafsanjani, A. Akbarzadeh, D. Pasini, Snapping mechanical metamaterials under tension, Adv. Mater. 27 (2015) 5931–5935.

[21] S. Shan, S. H. Kang, J. R. Raney, P. Wang, F. Lichen, F. Candido, J. A. Lewis, K. Bertoldi, Multistable architected materials for trapping elastic strain energy, Adv. Mater. 27 (2015) 4296–4301.

[22] D. Restrepo, N. D. Mankame, P. D. Zavattieri, Phase transforming cellular materials, Extreme Mech. Lett. 4 (2015) 52–60.

[23] T. Frenzel, C. Findeisen, M. Kadic, P. Gumbsch, M. Wegener, Tailored buckling microlattices as reusable light-weight shock absorbers, Adv. Mat. 28 (2016) 5865–5970.

[24] N. Kidambi, R. L. Harne, K.-W. Wang, Energy capture and storage in asymmetrically multistable modular structures inspired by skeletal muscle, Smart Mater. Struct. 26 (2017) 085011.

[25] C. Findeisen, J. Hohe, M. Kadic, P. Gumbsch, Characteristics of mechanical metamaterials based on buckling elements, J. Mech. Phys. Solids 102 (2017) 151–164.

[26] C. S. Ha, R. S. Lakes, M. E. Plesha, Design, fabrication, and analysis of lattice exhibiting energy absorption via snap-through behavior, Mater. Des. 141 (2018) 426–437.

[27] S. Zhu, X. Tan, B. Wang, S. Chen, J. Hu, L. Ma, L. Wu, Bio-inspired multistable metamaterials with reusable large deformation and ultra-high mechanical performance, Extreme Mech. Lett. 32 (2019) 100548.

[28] Z. Zhang, S. Pusateri, B. Xie, N. Hu, Tunable energy trapping through contact-induced snap-through buckling in strips with programmable imperfections, Extreme Mech. Lett. 37 (2020) 100732.

[29] C. Ren, D. Yang, H. Qin, Mechanical performance of multidirectional buckling-based negative stiffness metamaterials: an analytical and numerical study, Mater. 11 (2018) 1078.

[30] C. S. Ha, R. S. Lakes, M. E. Plesha, Cubic negative stiffness lattice structure for energy absorption: numerical and experimental studies, Int. J. Solids Struct. 178 (2019) 127–135.

[31] Y. Zhang, D. Restrepo, M. Velay-Lizancos, N. D. Mankame, P. D. Zavattieri, Energy dissipation in functionally two-dimensional phase transforming cellular materials, Sci. Rep. 9 (2019) 12581.

[32] S. Liu, A. I. Azad, R. Burgueño, Architected materials for tailorable shear behavior with energy dissipation, Extreme Mech. Lett. 28 (2019) 1–7.

[33] X. Tan, B. Wang, S. Zhu, S. Chen, K. Yao, P. Xu, L. Wu, Y. Sun, Novel multidirectional negative stiffness mechanical metamaterials, Smart Mater. Struct. 29 (2020) 015037.

[34] X. Tan, S. Chen, B. Wang, S. Zhu, L. Wu, Y. Sun, Design, fabrication, and characterization of multistable mechanical metamaterials for trapping energy, Extreme Mech. Lett. 28 (2019) 8–21.

[35] X. Tan, B. Wang, K. Yao, S. Zhu, S. Chen, P. Xu, L. Wang, Y. Sun, Novel multi-stable mechanical metamaterials for trapping energy through shear deformation, Int. J. Mech. Sci. 164 (2019) 105168.

[36] M. H. Fu, F. M. Liu, L. Hu, A novel category of 3D chiral material

[37] with negative Poisson's ratio, Compos. Sci. Technol. 160 (2018) 111–118.

[37] F. Auricchio, A. Bacigalupo, L. Gambarotta, M. Lepidi, S. Morganti, F. Vadala, A novel layered topology of auxetic materials based on the tetrachiral honeycomb microstructure, Mater. Des. 179 (2019) 107883.

[38] H. Ebrahimi, D. Mousanezhad, H. Nayeb-Hashemi, J. Norato, A. Vaziri, 3D cellular metamaterials with planar anti-chiral topology, Mater. Des. 145 (2018) 226–231.

[39] S. Eddins, Penrose Rhombus Tiling, 2019. URL: https://github.com/mathworks/penrose-tiling, Retrieved: August 2020.

[40] G. Miller, Automorphisms of the Dihedral Groups, Proc. Natl. Acad. Sci. 28 (1942) 368–371.